ARTICLES

Time-Resolved Dynamics of NO_2 in Its Conical Intersection Region

Benkang Liu,[†,‡] Jingyi Zhu,[†,‡] Bingxing Wang,[†,‡] Yanqiu Wang,[†] and Li Wang*[,†]

State Key Laboratory of Molecular Reaction Dynamics, Dalian Institute of Chemical Physics, Dalian 116023, China, and Graduate School of the Chinese Academy of Sciences, Beijing 100039, China

Received: July 24, 2009; Revised Manuscript Received: September 23, 2009

Photodissociation dynamics of NO_2 in its conical intersection region have been explored experimentally on a real-time scale by time-of-flight mass spectrometry. Excited at 400.6 nm and probed by 801.6 nm femtosecond laser pulses, different dynamical behaviors of both the parent ion NO_2^+ and the fragment ion NO^+ have been observed under parallel and perpendicular pump−probe laser polarization configurations. Distinct oscillations in NO_2^+ and NO^+ signals are observed when laser polarizations of pump and probe are perpendicular to each other, whereas the oscillations become blurry when the laser polarizations are parallel. The observed transient signals imply that the dissociation mechanism of NO_2 in the A^2B_2 excited state needed to be reconsidered. On the basis of our observation, Rydberg states play important roles in the ultrafast dissociation dynamics of NO_2.

1. Introduction

Since the original studies by Busch and Wilson in 1972,[1] the photodissociation of NO_2 via the A^2B_2 state has been extensively studied. The conical intersection[2] between its ground-state X^2A_1 and its first excited electronic state A^2B_2 results in the great complications in its spectra.[3] NO_2 has served as a benchmark polyatomic molecule for studies on unimolecular reaction dynamics, intramolecular vibrational redistribution, and vibronic coupling because of its rich and complex behavior despite its apparent simplicity as a triatomic molecule in past decades. Because of the small density of vibronic states close to the dissociation threshold (only a few states per inverse centimeter at 397.954 nm), the mechanism becomes complicated; that is, the photodissociation of NO_2 behaves statistically (internal vibrational redistribution prior to dissociation) or dynamically (state specific).[4]

NO_2 has been intensively explored on the vibronic coupling and non-Born−Oppenheimer dynamics in both the frequency domain[5,6] and time domain.[7,8] Whereas most essential questions about the frequency domain seem to be well understood, dynamical properties in the time domain still deserve detailed investigation. Numerous theoretical and experimental investigations in the time domain features of NO_2 have been reported in past decades.[9−20]

Time-resolved photoelectron−photoion coincidence experiments at 375 nm with laser intensity of $\sim 10^{12}$ W/cm^2 suggested the dominant dissociative process[11,12] to be a three-photon excitation to a repulsive state correlating to $NO(C^2\Pi) + O(^3P)$, followed by a one-photon ionization to yield $NO^+(X^1\Sigma^+) + O(^3P)$. At the same wavelength excitation, Singhal et al.[13] proposed that NO^+ came from one-photon excitation of NO_2, followed by electronic predissociation on the ground-state PES and subsequent three-photon ionization of NO with intensity of about 10^{13} W/cm^2.

Two-color fluorescence depletion spectroscopy experiments[14] suggested that the dominant dissociation pathway involved three-photon absorption of 400.6 nm light to an excited state of NO_2 (situated at 9.3 eV above the ground-state minimum). This state was estimated to dissociate to NO ($A^2\Sigma^+$, $v = 0$, 1, and 2) + $O(^3P)$ on a time scale no longer than 600 fs. In femtosecond time-resolved velocity map imaging experiments,[15] the NO^+ decay signal was attributed to two competitive mechanisms from the 400.6 nm pumped electronic state. The first was a fast process involving three-photon 400.6 nm absorption, followed by dissociative ionization by a subsequent 267.5 nm photon. The second was a slow process involving one-photon 400.6 nm absorption to the $^2B_2$ state, followed by two-photon dissociative ionization at 267.5 nm. The fast decay of NO^+ was suggested to be associated with a direct dissociation via the bending mode of the pumped state.[15]

Theoretically, Mahapatra et al.[7,16] applied the nonadiabatic wave packet method on realistic ab initio potential energy surfaces of NO_2 and explained the early experiments.[17] They figured out that the initial fast decay of the A^2B_2 diabatic population was followed by oscillation. Subsequently, two-color femtosecond experiments[15,18] indeed observed the slow NO^+ transient signal with an oscillatory component with a period of $\sim$600 fs, close to the first dissociation limit of NO_2. The observations had been suggested to be due to the average energy level spacing between the resonant levels of the A^2B_2/X^2A_1 states close to their conical intersection[15] or because of the free rotation of the oxygen atom around the NO molecule at large O−O distances.[18,19]

In a recent time-resolved coincidence imaging experiment,[20] fragmentation from both the ground state and the electronically excited a^3B_2 and b^3A_2 states of NO_2^+ had been observed. Slow statistical and fast direct fragmentation of NO_2^+ after prompt

* Corresponding author. E-mail: liwangye@dicp.ac.cn. Address: 457 Zhongshan Road, Dalian 116023, China. Fax: +86 411 84675584.
† Dalian Institute of Chemical Physics.
‡ Graduate School of the Chinese Academy of Sciences.

10.1021/jp907041a CCC: $40.75
Published on Web 10/14/2009

photoelectron ejection had been observed, leading to the formation of $NO^+ + O$. At short pump probe delay times, NO^+ was mainly produced via a $(3 \times 400) + (1 \times 267)$ nm excitation, whereas at longer delay times (>500 fs), NO^+ was produced via two multiphoton pathways. The dominant pathway was one 400 nm photon excitation, followed by two 267 nm photon absorption resulting in slow electrons and NO^+ ions. The second pathway was one 267 nm photon ionization of electronically and vibrationally excited NO ($A^2\Sigma$, $v = 1$) produced from the dissociation of NO_2 Rydberg states populated via three 400 nm photon excitation. No enhanced NO^+ signal was observed at the negative delay times corresponding to the 267 nm pump. However, at small negative delay times, a contribution of the 267 nm photons acting as pump was observed for the formation of NO_2^+, which was attributed to two 267 nm photon excitation to a 3d Rydberg state of NO_2, followed by one 400 nm photon ionization. A short-lived transient state was observed, populated by one 400 nm photon excitation. The third pathway results in a long-lived pump−probe signal that exhibits a signature of wavepacket motion. The wavepacket motion has been attributed to the accidental energy match of the 3.1 eV pump photon with the lowest neutral dissociation channel $NO(X^2\Pi) + O(^3P)$ near 3.18 eV. No pronounced oscillatory behavior was observed in the NO^+ transient profile.[20]

Obviously, the dynamics of NO_2 around its first conical intersection region is still unclear up-to-date. Recent experimental observations and theoretical descriptions had drawn different conclusions and explanations, as mentioned above. In this letter, we apply time-of-flight mass spectrometry and femtosecond pump−probe to readdress the dynamics of NO_2 around its first conical intersection. Despite the advantages of imaging techniques, there are some limitations and therefore disadvantages. Because of the limitation of inverse Abel transformation, the laser polarizations need be parallel to the image detector plane and perpendicular to the projection electric field in imaging the experimental setup, otherwise it is difficult to reconstruct the initial 3D velocity distributions of the charged particles from raw images. In some cases, such limitations may hinder the real information in photodissociation and ionization process, as we will show in this article. In this case, measurements of the product ions by time-of-flight mass spectrometry may provide direct insight information. In recent photoelectron−ion coincident[11,12,15,18,20] and direct current slice imaging experiments,[21] it becomes possible to avoid such limitations on the laser polarization geometries measurements. The kinetic energy and angular distributions for a molecular photodissociation may be obtained without the need to utilize inversion methods, such as the inverse Abel transform. For example, the polarization directions of both the pump and probe in ref 20 were perpendicular to the detector. In other experiments,[11,12,15,18] the polarization directions were parallel to the detector planes. However, up-to-date cross-polarization geometries have not been applied to the ultrafast dynamics of NO_2 by these methods. As we will present in this article, NO_2 shows different ultrafast behaviors in parallel-polarization and cross-polarization geometries.

In this article, we apply a 400.6 nm femtosecond laser to excite the NO_2 into its first conical intersection region and use femtosecond 801.6 and 267.5 nm lasers as probes to detect variations of NO_2 and its fragment product NO by multiphoton ionization. Our experimental results show different behaviors in different pump−probe polarizations setups and probe wavelengths. The lifetime constants are determined, and the decay dynamics of Rydberg states of NO_2 are discussed.

2. Experimental Section

Our homemade solid-state femtosecond laser system and the experimental setup had been described in detail elsewhere.[22] In brief, the laser system consists of a seed oscillator and amplifier with a stretcher and a compressor. The oscillator generates pulses with a temporal width of ~40 fs at a repetition rate of 110 MHz. After stretching and compression, the output light is centered at 801.6 nm (with fwhm of 14 nm) with energy of 160 mW average power, a temporal width of 60 fs, and a repetition rate of 20 Hz. The fundamental light is frequency doubled by a β-BaB_2O_4 crystal (BBO, type I) to produce the second harmonic generation (SHG) light, centered at 400.6 nm (with fwhm of 5.1 nm). For 267.5 nm light (with fwhm of 2.8 nm), the SHG and residual fundamental light are combined to generate the third harmonic generation (THG) light centered at 267.5 nm by a BBO crystal (type II). The wavelengths are measured by a high-resolution fiber optic spectrometer (model HR2000CG-UV-NIR, Ocean Optics, Inc.).

The fundamental light, SHG, and THG beams are focused by a fused quartz lens and passed into the chamber of a TOF mass spectrometer. We could vary the laser intensities at the focus spot by using different neutral density attenuators. The separated 801.6 or 267.5 nm from 400.6 nm is temporally delayed by a computer-controlled delay stage. The two laser beams are collinearly combined by a dichroic mirror and focused in the interaction region of the TOF mass spectrometer, respectively. The polarization direction of 400.6 nm is kept perpendicular to the axis of TOF and the molecular beam, whereas the polarization direction of 801.6 and 267.5 nm can be varied by a Berek compensator (model 5540).

The time-of-flight mass spectrometer used in our experiment is a typical Wiley−McLaren machine. The sample gas is expanded through a pulsed valve (General Valve, with 0.5 mm orifice) into the ionization accelerating region, 5 cm downstream from the nozzle. The ion optics consists of a typical velocity map imaging setup: repeller with open extractor and ground electrodes with 20 mm diameter central holes. Ions in this region are extracted and accelerated by a typical three-electrode system. After flying in a 40 cm field-free distance, ions are detected by a two-stage microchannel plate (MCP) detector at the end of the flight tube. The MCP signals are fed into a digital oscilloscope (Tektronix, TDS3054B, with 5 G/s sampling rate) GPIB interfaced with a computer. Each spectrum is averaged over 532 laser shots. In typical, each decay profile is averaged over >20 scans to yield a pump−probe transient.

The 2% NO_2/Ar sample molecules, mixed with a tiny amount of Xe for calibration, are expanded into TOF-MS through a pulsed valve (General Valve, with 0.5 mm orifice). There might be some N_2O_4 components in the sample gas mixture because of its high equilibrium constant, 0.15. However, this does not heavily affect measurements with the 400.6 nm pump because the absorption of NO_2 dominates at this wavelength. With the molecular beam on, the pressures of the source chamber and the flight chamber are maintained lower than 1.5×10^{-4} and 6×10^{-6} Pa, respectively.

3. Results

3.1. Typical Time-of-Flight Mass Spectra of NO_2. Figure 1 shows typical time-of-flight mass spectra of NO_2 obtained in our femtosecond pump−probe experiments (400.6 and 801.6 nm, with polarization direction perpendicular to each other). In the negative delay time range, one color (both 400.6 and 801.6 nm) produces negligible ion signals, as illustrated in Figure 1a. At zero delay time, in Figure 1b, NO^+ is about 2 times stronger

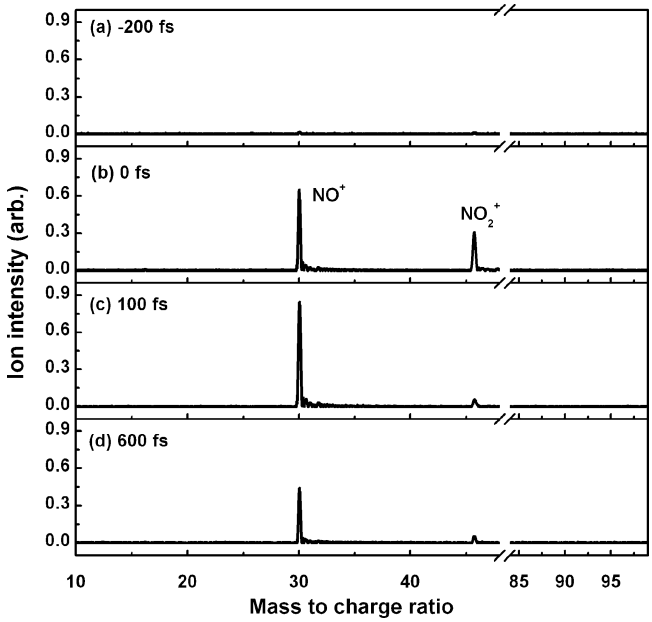

Figure 1. Time-of-flight mass spectra at different delay times. The polarization direction of 400.6 nm probe light is perpendicular to that of 801.6 nm probe light.

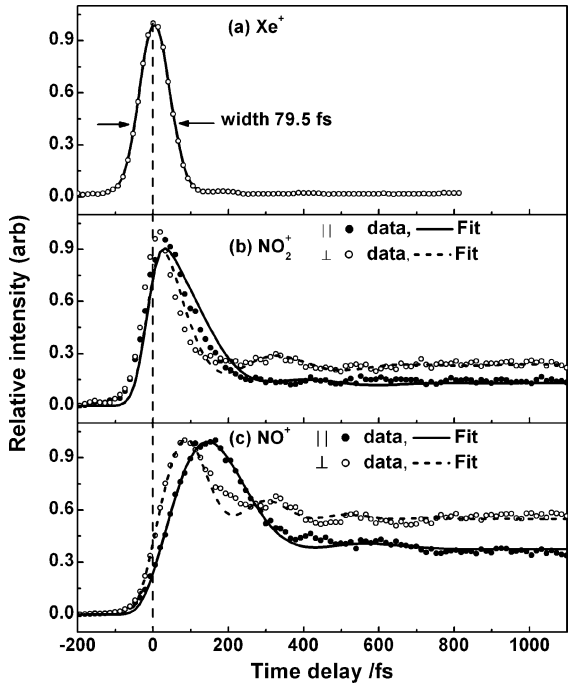

Figure 2. Transient profiles of NO_2^+ and NO^+ pumped by 400.6 nm and probed by 801.6 nm. (a) Xe^+ for determining the cross correlation function. (b) NO_2^+ in different polarization configuration experiments. (c) NO^+ in different polarization configuration experiments. Dashed line indicates the zero delay time, determined by Xe^+. ⊥ represents perpendicular polarization configuration, whereas || represents parallel polarization configuration. Solid dots and lines in parts b and c represent experimental and fitting results in parallel polarization configurations. Open circles and short dashed lines in parts b and c represent experimental and fitting results in perpendicular polarization configurations.

than NO_2^+, whereas NO_2^+ decreases much faster that NO^+, as shown in Figure 1c,d. No dimer ions, $N_2O_4^+$, or other ions, were observed. There may be a tiny N_2O_4 component in the supersonic molecular beam, but the contribution to the total ion signal would be negligible, as mentioned in ref 15.

3.2. Transient Profiles of NO_2^+ and NO^+ in 400.6 and 801.6 nm Experiments. Xe seeded in He was used for calibration of the pump−probe cross correlation, as illustrated in Figure 2a. The cross correlation between the pump and probe is a Gaussian function with a width of 79.5 fs. All transient profiles are deconvoluted by this function. Transient signals of NO_2^+ and NO^+ are recorded under different polarization setups of femtosecond 400.6 and 801.6 nm light, as illustrated in Figure 2b,c. When the polarization of 801.6 nm probe light is perpendicular to that of 400.6 nm pump light, pronounced oscillatory behaviors, in both NO^+ and NO_2^+ profiles, are observed in Figure 2b,c. The oscillation period in the NO^+ transient profile is ~220 fs. The maximum position of NO^+ is ~70 fs later than that of NO_2^+. Whereas the polarization of 801.6 nm is parallel to 400.6 nm, the oscillation almost disappears, as shown in Figure 2c, and the maximum position of the NO^+ transient profile presents itself ~150 fs later than that of NO_2^+ in Figure 2b.

Neither NO_2^+ nor NO^+ decay profiles in Figure 2b,c can be fitted by two exponential components. A cosine modulation component must be appended to one of the two exponential components. The fitting formula for NO_2^+ is given below

$$A_1 \times e^{-t/\tau_1} \times \left(1 + A_2 \times \cos\left(\frac{\pi \times \theta}{180} + \frac{2\pi \times t}{\tau_2}\right)\right) + A_3 \times e^{-t/\tau_3} + A_4 \quad (1)$$

The fitting formula for NO^+ is given in eq 2

$$A_1 \times e^{-t/\tau_1} \times \left(1 + A_2 \times \cos\left(\frac{\pi \times \theta}{180} + \frac{2\pi \times t}{\tau_2}\right)\right) + A_3 \times e^{-t/\tau_3} \times \left(1 + (1 - A_2) \times \cos\left(\frac{\pi \times (360 - \theta)}{180} + \frac{2\pi \times t}{\tau_2}\right)\right) + A_4 \quad (2)$$

The second item represents an exponential grown-up component. The best fitting parameters are listed in Table 1. The estimated errors of parameters in models 1 and 2 are constrained in 10%.

3.3. Transient Profiles of NO_2^+ and NO^+ in 400.6 and 267.5 nm Experiments. When the wavelength changes from 801.6 to 267.5 nm, different observations are obtained. As illustrated in Figure 3, in the negative delay time range, NO_2^+ shows enhanced signal, which means 267.5 nm is the pump source. No enhancement of NO^+ is obtained in the negative delay time range. Different from the behavior of NO_2^+, NO^+ is enhanced at positive delay time, which means 400.6 nm serves as the pump source. The maximum position of the NO^+ delay profile is the same as that of NO_2^+. Oscillatory behaviors with a period of ~500 fs in the NO^+ profile are observed, as illustrated in Figure 3, in the perpendicular polarization configuration experiment. Compared with the similar observations in 400.6 and 801.6 nm pump−probe experiments, the oscillatory behavior becomes unpronounced, as illustrated in Figure 4 in long delay time scale. Although the signal-to-noise of the oscillation is not enough for deconvolution analysis, the phenomenon is evident. One exponential decay model, eq 3, is applied for NO_2^+ profiles in the negative delay time region. The transient profiles of NO^+ are fitted by two exponential components in eq 4, one for decay and another one for grown-up. The fitting results are also listed in Table 1.

$$A_1 \times e^{-t/\tau_1} + A_3 \quad (3)$$

$$A_1 \times e^{-t/\tau_1} + A_2 \times (1 - e^{-t/\tau_2}) + A_3 \quad (4)$$

4. Discussion

In the experiments of 400.6 and 801.6 nm, both NO_2^+ and NO^+ signals are enhanced in the positive delay time ranges, as illustrated in Figures 1 and 2. In negative delay times, there are three possible excitation ways by multiple photon absorption of 801.6 nm. The first one is two-photon excitation to A^2B_2, which can be ionized by three 400.6 nm to produce NO_2^+. The second one is five photon excitation of 801.6 nm to the $3p\Pi_u$ Rydberg state, followed by two 400.6 nm photon ionization. The third one is six 801.6 nm photons absorption to the 5^2A_1 Rydberg state,[20] followed by one 400.6 nm photon ionization. Ionization detection via these intermediated Rydberg states is much more efficient than nonresonant multiphoton ionization. No enhancement of NO_2^+ or NO^+ in negative delay times means 400.6 nm light, as probe, is not intense enough for multiphoton ionization. This implies at positive delay times, where 400.6 nm serves as pump light, that the dominant excitation is due to one 400.6 nm absorption to the first conical intersection region between the ground state X^2A_1 and its first excited electronic state A^2B_2 of NO_2. In the 400.6 nm pump and 801.6 nm probe experiments, the decay profiles of NO_2^+ and NO^+ may be due to channels 1, 2, and 3, as marked in Figure 5. However, the dynamical behaviors will be slightly different for these three channels. Channel 1 will only produce NO_2^+, whereas NO^+ may be generated in channels 2 and 3. NO^+ from channel 2 will exhibit the same delay time dependence as NO_2^+ does, whereas NO^+ from channel 3 acts as an exponential grown component with a phase shift with respect to NO_2^+. The population of the excited state is fitted by a two-exponential component model, with one of them modulated by a cosine function to describe the fluctuations, as described in eq 13 in ref 19. The fitting results are illustrated in Figure 2 and listed in Table 1. The oscillatory period of the wave packet motion in the conical intersection, τ_2, is ~330 fs. The lifetime of the A^2B_2 state is ~150 fs, determined by τ_1 and τ_3. These lifetimes are also confirmed by the fitting results of NO^+ transient signals by eq 2, as illustrated in Figure 2 and listed in Table 1.

Interestingly, oscillation with a period of ~210 fs is observed in the NO^+ transient profile in Figure 2c in perpendicular polarization experiments, whereas in the parallel polarization experiments, the period becomes 2 times as long with a much worse signal to ratio. Such oscillatory behavior was reported in ref 15, with a period of ~600 fs. The oscillation was attributed to the wave packet motion in the conical intersection between the electronic ground state X^2A_1 and the first excited electronics state A^2B_2.[15] The origin of the oscillation behavior in NO^+ transient profile is still in debate. Theoretical calculation figured out that the initial population decayed at the rate of ~120 fs. The wiggle behaviors disappear when the vibronic coupling strength increases between the ground state X^2A_1 and the first excited electronic state A^2B_2,[16] and the oscillation had been suggested to be able to measure the average energy level spacing between the resonant levels of the A^2B_2/X^2A_1 states.[15] The authors of ref 18 tentatively attributed the oscillations to a free rotation of an oxygen atom around the NO molecule at large O−NO distances. Although our experimental results cannot tell the difference between these explanations, we prefer the mechanism of wavepacket motion along the conical intersection of the A^2B_2 state.[15,16] The oscillations of both NO_2^+ and NO^+ have the same phase angle, as shown in Figure 2b,c. If the oscillation of NO^+ was due to the free rotation of the oxygen at large O−NO distances, then the oscillation phase angle of NO_2^+ would be contrary to that of NO^+.

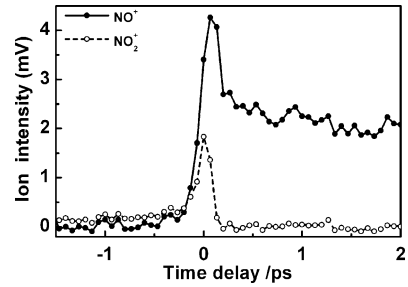

Figure 3. Transient profiles of NO_2^+ and NO^+ in 400.6 and 267.5 nm pump−probe experiments, where the polarization direction of 267.5 nm is parallel to the axis of TOF and perpendicular to the polarization direction of 400.6 nm.

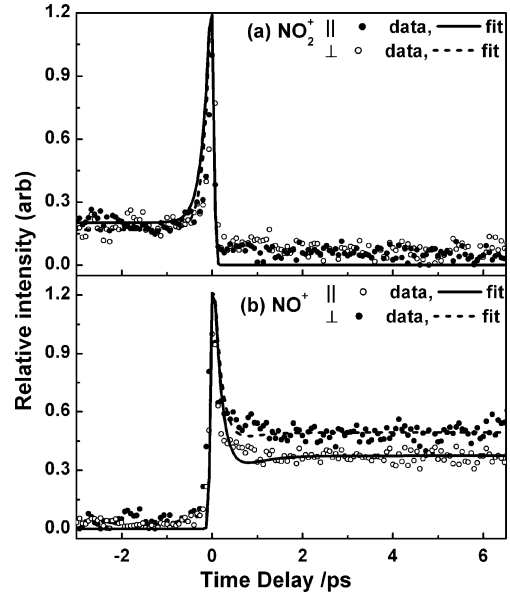

Figure 4. Transient profiles of (a) NO_2^+ and (b) NO^+ in 400.6 nm and 267.5 nm pump-probe experiments in long delay time scale.

TABLE 1: Fitting Parameters for NO_2^+ and NO^+ Transient Profiles[a]

		400.6 + 801.6 nm			400.6 + 267.5 nm	
	τ_1 (fs)	τ_2 (fs)	τ_3 (fs)	θ (deg)	τ_1 (fs)	τ_2 (fs)
NO_2^+ (⊥)[b]	179 (0.21)	333 (0.4)	144 (0.34)	140	143 (0.89)	
NO_2^+ (‖)[c]	179 (0.11)	333 (0.4)	122 (0.37)	40	168 (0.87)	
NO^+ (⊥)[b]	144 (0.23)	213 (0.53)	140 (−0.13)	130	184 (0.87)	380 (0.19)
NO^+ (‖)[c]	144 (0.45)	426 (0.39)	140 (−0.24)	140	192 (0.96)	480 (0.20)

[a] Numbers in brackets represent relative intensity of the corresponding component. [b] ⊥ represents perpendicular polarization configuration. [c] ‖ represents parallel polarization configuration.

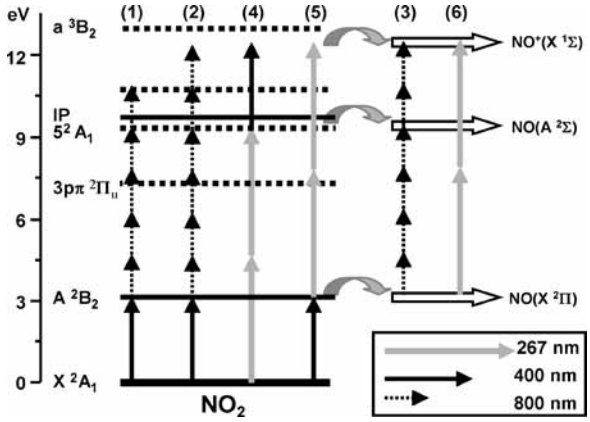

Figure 5. Photofragmentation and ionization channels of NO_2. One 267.5 nm photon is represented by a light gray arrow, the 400.6 nm photon is represented by a dark gray arrow, and the 801.6 nm photon is represented by a dashed dark arrow.

The oscillations become blurry while the polarization of 801.6 nm is parallel to 400.6 nm. Recent time-resolved investigations of photodynamics of NO_2 mainly concentrated on velocity mapping or coincidence imaging methods.[11,12,15,18] In these experiments, because of the kernel limitations of experiments, polarization directions need be parallel to the detector planes. As mentioned above, in such polarization configurations, the oscillatory behavior becomes blurry. This may explain why in these reports such oscillations were seldom observed.[20]

In the experiments of 267.5 and 400.6 nm pump−probe schedule, the oscillations are also observed, as illustrated in Figure 3. Channel 4 corresponds to the enhancement of NO_2^+ in the negative delay times, that is, two 267.5 nm photons excite NO_2 from ground electronics state to the high Rydberg state, 5^2A_1 and followed by one 400.6 nm photon ionization. As listed in Table 1, the lifetime of NO_2 in the 5^2A_1 Rydberg state is ~150 fs.

Channels 5 and 6 correspond to the transient profiles of NO^+ and NO_2^+ in the positive delay times. One 400.6 nm photon projects NO_2 into the A^2B_2 state, from which NO_2 may dissociate into NO ($X^2\Pi$) through the conical intersection. The neutral dissociation product NO is then ionized by two 267.5 nm photons. The only possible channel for producing NO_2^+ is channel 5. Enhancement of NO_2^+ in one 400.6 nm photon excitation region had been observed,[15] but is much smaller than that in the negative delay time region. NO^+ produced from channel 5 follows the same behavior as NO_2^+, that is, decay exponential component. An exponential grown-up component will correspond to the NO^+ transient profile generated from channel 6. On the basis of our experimental observation and the fitting results, NO^+ may be produced via both channels 5 and 6. The fitting models employed in simulating our experimental results are based on the above discussions. We use a two-exponential component model, in which one is for grown and another one is for fast decay instead of the two-decay exponential model in ref 15. The results imply that the model is reasonable. As illustrated in Figure 5, the first excited state, A^2B_2, plays a key role in producing NO^+ signals, in both 801.6 and 267.5 nm experiments.

Another obvious phenomenon is that enhancement of NO^+, either in 400.6 and 801.6 nm experiments or in 400.6 and 267.5 nm experiments (Figure 4), is much stronger in the perpendicular polarization configuration than in the parallel polarization configuration. This may also be the reason the oscillation can be observed evidently in perpendicular polarization configuration. The equilibrium bond angles between two N−O bonds of NO_2 in the ground-state X^2A_1 and the first excited electronic state A^2B_2 are 134 and 102°, respectively.[23] The NO_2^+ electronics ground state is of linear geometry. The A^2B_2 state is known to undergo internal conversion back to the ground state via a conical intersection at a bending angle of 113°.[24] In the relative intense laser field of femtosecond pump light field, the structure of the molecular NO_2 is deformed, and bond angle will increase toward a linear configuration.[16] The deformed NO_2 is excited to the bending mode vibration, leading to a fast dissociation to NO.[15] Suppose the transition dipole moment is along the C_{2v} symmetry axis of NO_2, the excited NO_2 will change to linear geometry, whereas the fragment NO leaves the parent molecule with nearly perpendicular momentum to the initial excitation. This may explain the observation that the enhancement of NO^+ is much stronger in perpendicular polarization configuration than in parallel polarization configuration.

In the comparison between 801.6 and 267.5 nm experiments, both the signal intensity enhancement and the oscillation of NO^+ are stronger in 801.6 nm experiments than in 267.5 nm experiments. As illustrated in Figure 5, the difference in these two cases with 400.6 nm as the pump light is the Rydberg state, 5^2A_1, as the intermediated state in the 801.6 nm probe schedule. The existence of this intermediated state in the 801.6 nm multiphoton ionization detection schedule enhances the ionization efficiency. This also occurs in NO_2^+ in the positive delay times.

5. Conclusions

Time-resolved photodissociation dynamics of NO_2 are investigated by using time-flight mass spectrometry. In 400.6 and 801.6 nm pump−probe experiments, the dominant excitation is one 400.6 nm photon absorption to the first excited electronic state A^2B_2, the first conical intersection region. Part of the population in the A^2B_2 state will dissociate into neutral NO. Five 801.6 nm photon ionizations of this neutral NO fragment will exhibit exponential grown behavior. Residual NO_2 in A^2B_2 is ionized by five or six 801.6 nm photon absorptions via 3 $p\pi^2\Pi_u$ or 5^2A_1 Rydberg states. The ionic fragment NO^+ from this channel follows the same two-decay exponential model as NO_2^+.

In 400.6 and 267.5 nm pump−probe experiments, two 267.5 nm photon absorption to the 5^2A_1 Rydberg state followed by one 400.6 nm photon ionization mainly results in enhanced NO_2^+ signal in the negative delay times in our experiments. The enhanced NO^+ signals are predominantly produced from the A^2B_2 state, populated by one 400.6 nm photon excitation and followed by two 267.5 nm photon ionization, either from the dissociative ionization of NO_2 or from the ionization of the dissociation neutral NO via the conical intersection. The NO^+ from the first pathway follows the same dynamical behavior as NO_2^+, that is, exponential decay mixed with oscillatory decay. The NO^+ from the second pathway exhibits exponential grown behavior. The fitting results indicate that both of these two channels are involved in our experiments.

Differences in enhancements and oscillations of NO^+ between experiments of 801.6 and 267.5 nm may be the indicator of the involvement of the 5^2A_1 Rydberg state as intermediated state in 801.6 nm multiphoton probing. Efficiency of multiphoton ionization detection via such intermediated states will be enhanced. The same oscillation phase angles and periods of NO_2^+ and NO^+ prefer the mechanism of wavepacket motion along the conical intersection of the A^2B_2 state.

Acknowledgment. We would like to acknowledge the financial support from the National Natural Science Foundation of China (grant nos. 20633070 and 20473090).

References and Notes

(1) Busch, G. E.; Wilson, K. R. *J. Chem. Phys.* **1972**, *56*, 3626.
(2) Hirsch, G.; Buenker, R. J.; Petrongolo, C. *Mol. Phys.* **1991**, *73*, 1085.
(3) Delon, A.; Jost, R.; Jacon, M. *J. Chem. Phys.* **2001**, *114*, 331.
(4) Matthews, S. J.; Willitsch, S.; Softley, T. P. *Phys. Chem. Chem. Phys.* **2007**, *9*, 5656.
(5) Haller, E.; Koppel, H.; Cederbaum, L. S. *J. Mol. Spectrosc.* **1985**, *111*, 377.
(6) Joyeux, M.; Jost, R.; Lombardi, M. *J. Chem. Phys.* **2003**, *119*, 5923.
(7) Manthe, U.; Koppel, H. *J. Chem. Phys.* **1990**, *93*, 1658.
(8) Sanrey, M.; Joyeux, M. *J. Chem. Phys.* **2006**, *125*, 014304.
(9) Arasaki, Y.; Takatsuka, K. *Chem. Phys.* **2007**, *338*, 175.
(10) Wilkinson, Iain; Whitaker, B. J. *J. Chem. Phys.* **2008**, *129*, 154312.
(11) Davies, J. A.; LeClaire, J. E.; Continetti, R. E.; Hayden, C. C. *J. Chem. Phys.* **1999**, *111*, 1.
(12) Davies, J. A.; Continetti, R. E.; Chandler, D. W.; Hayden, C. C. *Phys. Rev. Lett.* **2000**, *84*, 5983.
(13) Singhal, R. P.; Kilic, H. S.; Ledingham, K. W. D.; McCanny, T.; Peng, W. X.; Smith, D. J.; Kosmidis, C.; Langley, A. J.; Taday, P. F. *Chem. Phys. Lett.* **1998**, *292*, 643.
(14) Lopez-Martens, R. B.; Schmidt, T. W.; Roberts, G. *J. Chem. Phys.* **1999**, *111*, 7183.
(15) Eppink, A. T. J. B.; Whitaker, B. J.; Gloaguen, E.; Soep, B.; Coroiu, A. M.; Parker, D. H. *J. Chem. Phys.* **2004**, *121*, 7776.
(16) Mahapatra, S.; Koppel, H.; Cederbaum, L. S.; Stampfub, P.; Wenzel, W. *Chem. Phys.* **2000**, *259*, 211.
(17) Weaver, A.; Metz, R. B.; Bradforth, S. E.; Neumark, D. M. *J. Chem. Phys.* **1989**, *90*, 2070.
(18) Form, N. T.; Whitaker, B. J.; Poisson, L.; Soep, B. *Phys. Chem. Chem. Phys.* **2006**, *8*, 2925.
(19) Sanrey, M.; Joyeux, M. *J. Chem. Phys.* **2007**, *126*, 074301.
(20) Vredenborg, A.; Roeterdink, W. G.; Janssen, M. H. M. *J. Chem. Phys.* **2008**, *128*, 204311.
(21) Townsend, D.; Minitti, M. P.; Suits, A. G. *Rev. Sci. Instrum.* **2003**, *74*, 2530.
(22) Yuan, L. W.; Zhu, J. Y.; Wang, Y. Q.; Wang, L.; Bai, J. L.; He, G. Z. *Chem. Phys. Lett.* **2005**, *410*, 352.
(23) Gillispie, G. D.; Khan, A. U. *J. Chem. Phys.* **1976**, *65*, 1624.
(24) Schryber, J. H.; Polyansky, O. L.; Jensen, P.; Tennyson, J. *J. Mol. Spectrosc.* **1997**, *185*, 234.

JP907041A